JOURNAL OF GUIDANCE, CONTROL, AND DYNAMICS
Vol. 18, No. 4, July–August 1995

Human-in-the-Loop Evaluation of Remote Manipulator System Active Damping Augmentation

Martha E. Demeo*
ViGYAN, Inc., Hampton, Virginia 23666
Michael G. Gilbert† and Michael A. Scott‡
NASA Langley Research Center, Hampton, Virginia 23681
Janet A. Lepanto§
Charles Stark Draper Laboratory, Inc., Cambridge, Massachusetts 02139
Elizabeth M. Bains¶
NASA Johnson Space Center, Houston, Texas 77058
and
Mary C. Jensen††
Lockheed Engineering and Sciences Company, Inc., Houston, Texas 77058

This paper describes the application of controls-structures integration technology to benefit the on-orbit performance of the Space Shuttle remote manipulator system. Called active damping augmentation, the goal is to reduce the vibration decay time of the remote manipulator system following normal payload maneuvers and operations. Simulation of active damping augmentation was conducted in a real-time human-in-the-loop simulation of the remote manipulator system with the objective of obtaining qualitative and quantitative measurements of operational performance improvements from astronaut operators. Sensing of vibratory motions was simulated using a three-axis accelerometer mounted at the end of the lower boom of the remote manipulator system. The sensed motions were used in a feedback control law to generate commands to the remote manipulator system joint servo mechanisms which reduced the unwanted oscillations. Active damping of the remote manipulator system with an attached 3990-lb payload was successfully demonstrated. Six astronaut operators examined the performance of an active damping augmentation control law following payload maneuvers and Shuttle thruster firings. Significant reductions in the dynamic response were observed and investigation of performance benefits with heavier attached payloads was recommended.

Nomenclature

A = dynamics matrix
B = control distribution matrix
C = observation matrix
D = control feedthrough matrix
G = control gain matrix
H = observer gain
J = cost function
K = solution matrix of Riccati equation
k = index
m = number of model inputs and outputs
n = identified model order
Q = output weighting matrix
R = control weighting matrix
$\boldsymbol{u}(k)$ = discrete time input vector
$\boldsymbol{x}(k)$ = discrete time state vector
$\hat{x}(k)$ = discrete time estimate of the state $\boldsymbol{x}(k)$
$\boldsymbol{y}(k)$ = discrete time output vector

Subscripts

c = compensator
g = global
ψ = identified linear model

Presented as Paper 93-3875 at the AIAA Guidance, Navigation, and Control Conference, Monterey, CA, Aug. 9–11, 1993; received Sept. 9, 1993; revision received July 17, 1994; accepted for publication July 22, 1994.

*Research Engineer, Multidisciplinary Research Group. Senior Member AIAA.
†Assistant Branch Head, Spacecraft Dynamics Branch. Senior Member AIAA.
‡Aerospace Engineer, Spacecraft Controls Branch. Member AIAA.
§Senior Technical Staff, Control and Decision Systems Division.
¶Deputy Chief, Simulations Systems Branch. Associate Fellow AIAA.
††Test and Validation Engineer, Simulation Development Department.

I. Introduction

THE Space Shuttle uses the six-joint, 50-ft-long anthropomorphic remote manipulator system (RMS) for the on-orbit maneuvering, deployment, and retrieval of satellites, scientific payloads, and (occasionally) space walking astronauts. The RMS is commanded from the aft flight deck of the Space Shuttle using rotational and translational hand controllers and a control panel. Using various operational modes, joint angle readouts, remote cameras, and visual sightings, Shuttle astronauts maneuver the RMS to grapple and precisely position payloads for berthing, unberthing, and deployment.

For various reasons, including stopping distance and easily excited RMS dynamics, the maneuvering of RMS attached payloads is intentionally slow and deliberate. To avoid exciting undesired dynamic response, astronauts operating the RMS are trained to use hand controller inputs which reduce RMS start and stop transients and to wait between hand controller inputs for transient motions to decay. The likelihood of inducing undesired start and stop transients and the time needed for such motion to decay both increase in proportion to payload mass. As a result, on-orbit payload operations typically take many hours to complete, particularly in the case of large payloads.

The use of controls-structures integration (CSI) technology to improve RMS operational timelines by actively increasing the damping

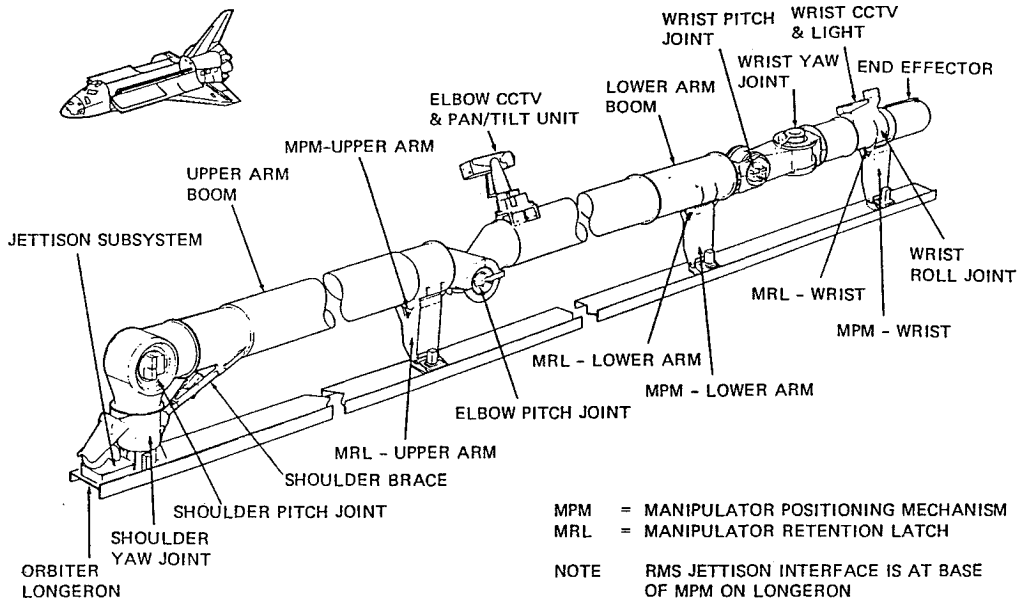

Fig. 1 Remote manipulator system.

of RMS response has been investigated. This study, known as RMS active damping augmentation (ADA), has been a multiyear effort involving both government and industry participants. The intent of this CSI technology application is to reduce both the peak response and the settling time of RMS stop transients. Benefits of ADA to RMS performance include less wait time between commands, loads reduction, improved disturbance rejection due to Shuttle thruster firings, and improved payload positioning steady-state error.

This paper describes recent human-in-the-loop testing of ADA in the systems engineering simulator (SES) at the NASA Johnson Space Center. The purpose of this testing was to obtain qualitative and quantitative ADA performance data from trained RMS operator astronauts. This data was needed to assess the benefits of RMS ADA and to determine whether the performance improvements merit on-orbit flight demonstration.

Section II provides a summary of the RMS system, the technical approach, study parameters used in the development of ADA control laws, and the objectives and goals for SES testing. Sections III and IV cover the development of the ADA control laws using identified system mathematical models and various control law design techniques. Section V describes the implementation of ADA in the SES RMS simulator, and Sec. VI presents the results of the testing.

II. Remote Manipulator System Active Damping Augmentation System

Remote Manipulator System Description

The RMS is mounted to the port longeron of the Space Shuttle cargo bay. From this attachment point, the arm is comprised of two single-degree-of-freedom (DOF) shoulder joints (yaw and pitch), a 21-ft-long upper boom, a single-DOF elbow pitch joint, a 23-ft-long lower boom, 3 single-DOF wrist joints (pitch, yaw, roll), and a snare type end effector capable of mating with a payload mounted grapple fixture (Fig. 1). Encoders and tachometers reside at each of the six joint servos to measure joint position and joint rate, respectively.[1]

The arm is telerobotically controlled from the aft cockpit of the Shuttle by translational and rotational hand controllers and control panel command inputs. Joint rate commands are sent from software algorithms resident in the Shuttle general purpose computer (GPC) to the six independent joint servos by way of a manipulator control interface unit (MCIU). The joint rate commands generated in the GPC depend on the selected operational mode. These modes include a single-joint mode, four manual modes, and an automatic mode. The output rate commands are limited in the GPC according to arm loading conditions, i.e., payload mass. When not being commanded to move, the arm is held in place by a position-hold function, zero-rate-command hold, or brakes. In position hold, joint rate commands

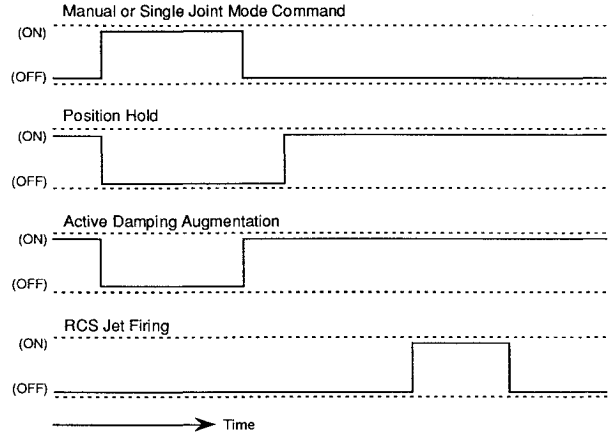

Fig. 2 ADA implementation logic.

are generated to maintain the commanded position of the arm based on feedback of joint angles. In zero-rate-command hold, the joint rate commands are set to zero. When the brakes are engaged, externally applied torques are opposed by brake static friction.[2]

Technical Approach to Active Damping Augmentation

The selected approach to active damping augmentation of the RMS is to drive selected joints to suppress motion sensed by a three-axis accelerometer mounted on the RMS using a feedback control law. Previous work[3,4] described the use of the joint servo motors as actuators, the need for acceleration sensing, and possible control laws.

The strategy for implementing the ADA compensators was based on two ground rules. The first ground rule was that ADA not change the way the RMS feels to a trained operator. As a result, it was decided that ADA be activated following the removal of RMS single-joint and manual mode commands. As shown in Fig. 2, ADA is initiated in single mode when the single drive switch is returned to detent. In manual mode, ADA is activated when the hand controllers are returned to detent. ADA remains on until the next maneuver command is initiated. When the joint rates fall below a threshold value and the position-hold mode is entered, joint rate commands from the ADA compensator and the position-hold function are summed. With this implementation, active damping of external disturbances, such as Shuttle reaction control system (RCS) thruster firings, can also be achieved. The second ground rule was that changes to the RMS software to accommodate ADA

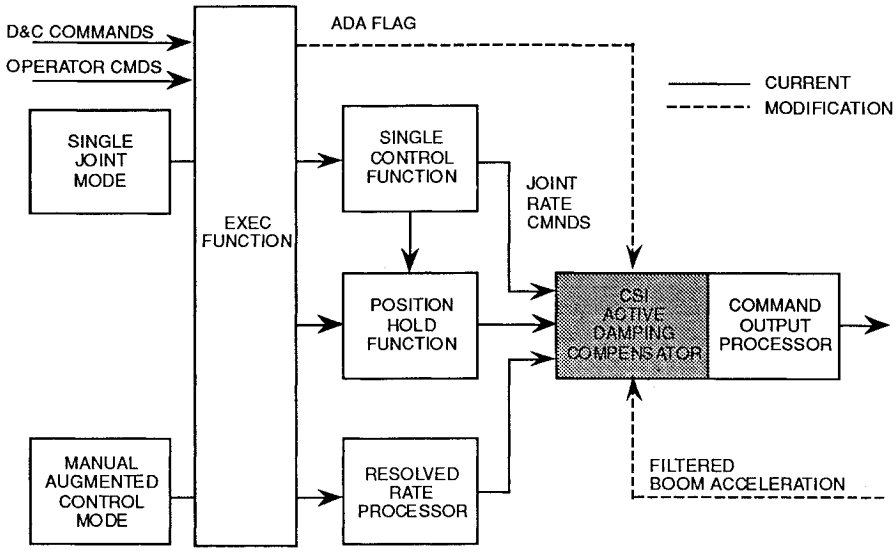

Fig. 3 CSI controller implementation.

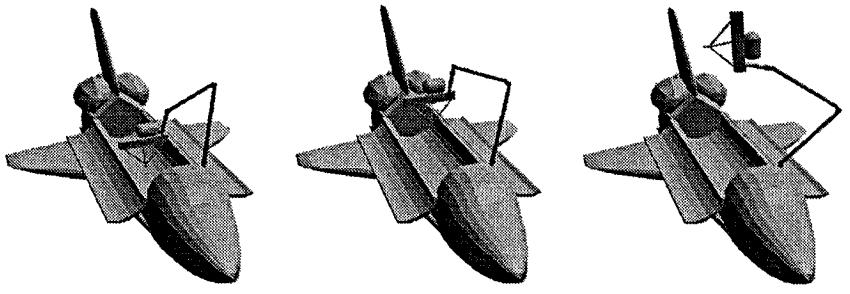

Fig. 4 RMS ADA study configurations.

be localized to the greatest extent possible and adhere to the nominal health and safety monitoring of the RMS including the payload dependent joint rate limits. As shown in Fig. 3, the ADA algorithm was appended to the front of the RMS software command output processor. Minor modifications were also made to other software modules. The joint rate limits were explicitly imposed in the ADA compensator output as is typically performed elsewhere in RMS software.

A key consideration in the implementation of ADA control laws in the Shuttle GPC was to minimize the gain scheduling necessary to accommodate the large motions of the RMS. To achieve this goal, several different robust control law design methods were used to establish candidate ADA control laws. The approach was to develop and test point-design control laws (control laws designed for a particular RMS configuration and payload) in the SES for damping performance and robustness to configuration changes. Several candidate control laws from this group were then further refined to achieve stable performance over a set of possible configurations and used for the astronaut evaluations reported in this paper. More detail on the design of the ADA controls laws is given in Secs. III and IV.

Study Parameters

Payload Definition

The payload chosen for this study was the 3990-lb Shuttle pallet satellite (SPAS-02). This carrier is a typical midrange mass payload and is a reconfigured version of the SPAS-01 payload used in previous ADA studies.[4] The SPAS-02 payload features a grapple fixture at an angle of 15 deg from vertical and offset from the payload center-of-gravity by 5.8 ft.

Sensor/Actuator Definition

A three-axis accelerometer mounted at the grapple-fixture end of the lower boom was selected to sense the RMS vibration and provide feedback signals for ADA. Results from an initial feasibility study determined that acceleration feedback had significantly more damping potential than feedback of the joint tachometer signals.[3] The location of the accelerometer, inboard of the wrist joints, was selected to minimize the number of transformations required to resolve the acceleration signal. The actuators selected for active damping include the shoulder yaw, shoulder pitch, and elbow pitch joint servos motors.

Baseline Remote Manipulator System Configuration Definition

Three point-design arm configurations were selected from the SPAS-02 mission. They include an unberth, low hover, and deploy configuration as depicted in Fig. 4.

III. System Identification

Description of Observer/Kalman Filter Identification

For the purposes of ADA control law design, linear multi-input, multi-output state-space models were derived from simulated response data using the observer/Kalman filter identification algorithm (OKID).[5,6] This system identification methodology allows a state-space model and corresponding observer to be identified directly from time response data.

Systems Engineering Simulator Preprogrammed Test Inputs

Response data of the RMS for use in system identification were generated in the SES using preprogrammed test inputs (PTIs). Three PTIs were run for each of the three arm configurations. These consisted of positive and negative full-scale rate command pulses to each of the shoulder yaw, shoulder pitch, and elbow pitch joint servos. The width of the command pulses was selected to correspond to the half-period of the fundamental mode of the arm with the attached 3990-lb payload. This method of excitation was chosen over random noise or band-limited noise inputs to specifically excite the low-frequency modes that needed to be identified.

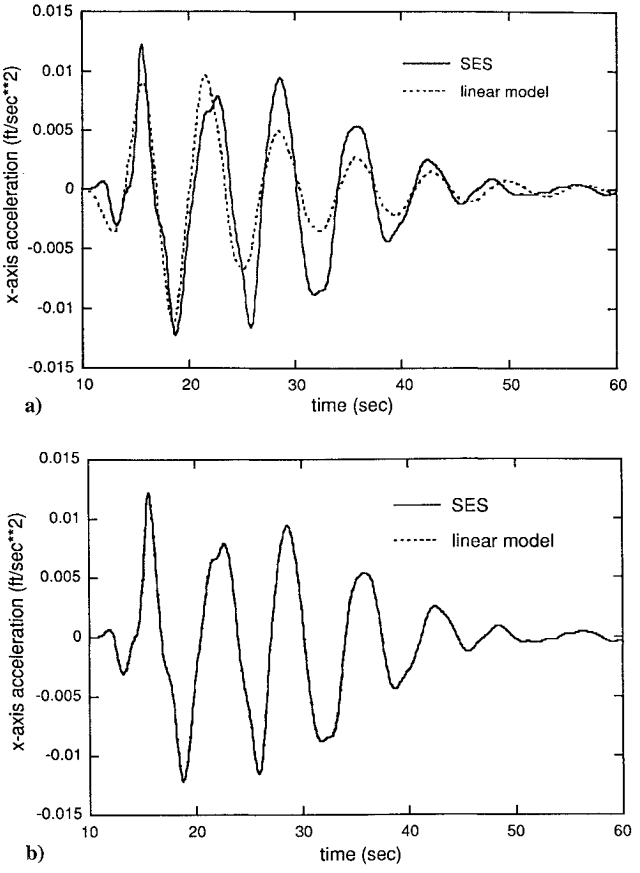

Fig. 5 Typical system identification results a) without observer and b) with observer.

Linear Models

The aggregated input data for the OKID algorithm were the joint rate commands to the shoulder yaw, shoulder pitch, and elbow pitch servos, and the aggregated output data were the simulated triaxial boom acceleration signals. These acceleration signals were filtered using a third-order lowpass Butterworth filter with a break frequency of 0.18 Hz to minimize aliasing, reduce effects of noise, and to provide a frequency-weighted model.

The identified discrete linear time-invariant plant model includes the system dynamics and the filters in the form

$$\begin{aligned} \boldsymbol{x}(k+1) &= A\boldsymbol{x}(k) + B\boldsymbol{u}(k) \\ \boldsymbol{y}(k) &= C\boldsymbol{x}(k) + D\boldsymbol{u}(k) \end{aligned} \tag{1}$$

where $\boldsymbol{x}(k) \in R^n$, $\boldsymbol{u}(k) \in R^m$, and $\boldsymbol{y}(k) \in R^m$. The identified model order, n, is specified by the user as part of the identification process.[7]

The corresponding identified observer obtained from the OKID algorithm is of the form

$$\begin{aligned} \hat{\boldsymbol{x}}(k+1) &= A\hat{\boldsymbol{x}}(k) + B\boldsymbol{u}(k) - H[\boldsymbol{y}(k) - \hat{\boldsymbol{y}}(k)] \\ \hat{\boldsymbol{y}}(k) &= C\hat{\boldsymbol{x}}(k) + D\boldsymbol{u}(k) \end{aligned} \tag{2}$$

Augmenting the plant model with this observer yields

$$\begin{aligned} \hat{\boldsymbol{x}}(k+1) &= (A + HC)\hat{\boldsymbol{x}}(k) + [B + HD - H]\begin{bmatrix} \boldsymbol{u}(k) \\ \boldsymbol{y}(k) \end{bmatrix} \\ \hat{\boldsymbol{y}}(k) &= C\hat{\boldsymbol{x}}(k) + D\boldsymbol{u}(k) \end{aligned} \tag{3}$$

This augmented system definition was used directly in ADA compensator design. For each of the point-design arm configurations, 12th-order linear models were identified that sufficiently captured the low-frequency modes of the RMS/payload system. Typical system identification results are shown in Fig. 5. The figure depicts the y-axis (filtered) acceleration predicted by the identified linear model (dashed line) vs the response data from the SES (solid line) with and without the identified observer.

IV. Control Law Design and Evaluation

Objectives and Approach

The objectives of the ADA control law designs were to damp oscillations of the RMS system, to reduce the vibration decay time of the RMS following normal payload maneuvers and operations, and to be robust to changes in arm configurations. Two types of control laws were developed. The first type were point-design compensators in which system nonlinearities (e.g., flexibility of structural members, joint servo and motor dynamics, gearbox compliance, and data transfer delays) were modeled as white noise parts of the identified linear models, specifically in the observer noise properties. The second type was a single global controller that addressed the kinematic nonlinearities of large joint angle maneuvers.

The approach taken in the ADA compensator development was to start with control laws designed to operate at each of three point-design configurations and work toward one that performed over the range of arm configurations. The method explored in the design of these, so-called, global controllers was direct gradient-based optimization (GBO). The sections that follow provide descriptions of the linear quadratic regulator (LQR)-based point designs and the gradient-based global controller designs.

Linear Quadratic Regulator and Observer Design

A set of initial point-design (RMS configuration dependent) ADA compensators were obtained using a frequency-weighted LQR approach[8,9] and the identified (nonoptimal) observer to provide state estimates. The motivation for this choice was that it easily handles the multi-input, multi-output (MIMO) system and that it allows for tradeoffs between end-point acceleration/damping response and available actuator power. The sampling period for the design presented was selected to correspond to the 12.5-Hz rate of the GPC.

This design employed the discrete optimal control law,

$$\boldsymbol{u}(k) = -G\hat{\boldsymbol{x}}(k) \tag{4}$$

where the control gain matrix G is defined as

$$G = (R + B'KB)^{-1}B'KA \tag{5}$$

and $K = K' > 0$ is an $n \times n$ solution matrix of the discrete algebraic Riccati equation. The regulator gain found minimized the following quadratic cost function subject to the dynamic constraints imposed by the open-loop dynamics:

$$J_i = \sum_{k=0}^{\infty} [\boldsymbol{x}'(k)Q^*\boldsymbol{x}(k) + \boldsymbol{u}'(k)R^*\boldsymbol{u}(k)] \tag{6}$$

with $Q^* = C'QC$ and $R^* = D'QD + R$. The output weighting matrix Q^* and the control weighting matrix R^* were assumed to be symmetric and positive semidefinite. Numerical values of Q and R were determined using an iterative design procedure on the linear model which avoided actuator saturation. That is, the required control was less than the payload dependent joint rate limits (e.g., for the shoulder joints, this coarse mode limit was 0.7083 deg/s).

The MIMO ADA compensator equation is of the form

$$\begin{aligned} \hat{\boldsymbol{x}}(k+1) &= (A + HC - BG + HDG)\hat{\boldsymbol{x}}(k) - H\boldsymbol{y}(k) \\ \boldsymbol{u}(k) &= -G\hat{\boldsymbol{x}}(k) \end{aligned} \tag{7}$$

The resulting closed-loop system is written as

$$\begin{bmatrix} \boldsymbol{x}(k+1) \\ \hat{\boldsymbol{x}}(k+1) \end{bmatrix} = \begin{bmatrix} A & -BG \\ -HC & A + HC - BG \end{bmatrix}\begin{bmatrix} \boldsymbol{x}(k) \\ \hat{\boldsymbol{x}}(k) \end{bmatrix} + \begin{bmatrix} B \\ -HD \end{bmatrix}\boldsymbol{u}(k) \tag{8}$$

$$\boldsymbol{y}(k) = [\,C \;\; -DG\,]\begin{bmatrix} \boldsymbol{x}(k) \\ \hat{\boldsymbol{x}}(k) \end{bmatrix} + [D]\boldsymbol{u}(k)$$

Gradient-Based Optimization

The gradient-based global controller design was developed using a quasi-Newton numerical optimizer and a finite time numerical calculation of a quadratic cost function. The objective was to damp oscillations of the RMS system over a wide range of arm orientations using a single global control law. The starting point for this optimization scheme was an LQR-based compensator designed about the low-hover configuration. This initial compensator was then optimized with respect to the three point-design linear models.

The LQR point-design, described earlier, optimized a controller gain based on the dynamic knowledge of one plant configuration. Thus, the solution involved minimizing a single quadratic cost function. The LQR point-design controller matrices, defined in Eq. (7), were chosen as the initial values in the optimization routine. Although it was desirable for the initial controller matrices to stabilize all three plants, it was not necessary for convergence of the optimization algorithm.

The approach taken for the global controller employed gradient-based optimization techniques to minimize the sum of three quadratic cost functions computed using three independent models of the RMS in the defined orientations. The cost function is

$$J_g = \sum_{i=0}^{N} J_i \tag{9}$$

To compute the global cost J_g, a step input was applied to each of the three closed-loop linear models. The scalar cost J_i, is determined by inserting the finite time sequence of the resulting control input $\boldsymbol{u}$ and closed-loop response output $\boldsymbol{y}$ of each of the three linear models (corresponding to the three arm configurations) into Eq. (4). The input used in this optimization was a 3.5-s step input. The duration of the step input was tailored to optimize the controller for the frequency band of interest. The duration of the time sequence N was chosen such that all plant transients were damped sufficiently. The algorithm minimized the multiplant cost J_g by varying the elements of the global gain matrix G_g using a quasi-Newton numerical optimization routine.

Nonreal-Time Evaluation

Preliminary performance evaluations of the ADA point-design and global control laws were conducted using the identified linear models and, additionally, two nonlinear simulations of the RMS. The two nonlinear simulations were the Draper RMS simulation (DRS) and a modified version of the DRS called the SES/DRS. The DRS is a high-fidelity nonreal-time simulation of the RMS which has been validated against flight data.[10] The simulation includes models of a rigid Shuttle, the seven links of the RMS, a rigid payload, and detailed models of the RMS joint servos and control software. The SES/DRS is a version of the DRS that mimics the dynamics of the real-time SES.

Several evaluations were conducted with both the DRS and the SES/DRS to address maximum valid arm motion ranges, stability margins, variations between DRS and SES dynamics, gain scheduling, loads reductions, effects of RMS nonlinearities, and computer signal time delays.

V. Real-Time Simulation

Description of Systems Engineering Simulator

The SES is a real-time, human- and/or hardware-in-the-loop simulator located at the NASA Johnson Space Center. It supports developmental testing and operations for Space Shuttle, Space Station Freedom, and advanced programs. Developmental testing typically includes evaluation of areas where human/machine interaction is a significant consideration. Operations support includes engineering evaluation, mission design and training, and real-time mission support when required.

Testing in the SES is routinely performed in one or more of the available cockpit mockups. These mockups provide functional displays and controls for human-in-the-loop interaction with a computer simulated dynamic environment. Out-the-window views and closed-circuit television camera views, generated by electronic scene generators, give the operator visual cues that would be available in the environment being simulated.

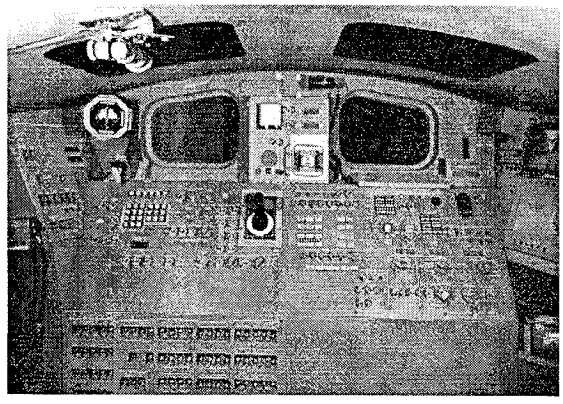

Fig. 6 SES Shuttle aft flight deck.

The SES consists of two simulators: an ascent/entry simulator with Shuttle forward cockpit and an on-orbit simulator with four cockpits/workstations that can be used independently or in an integrated simulation. Multiple scene generators can drive different eyepoints of one cockpit or can drive eyepoints in different cockpits. The on-orbit simulation with the Shuttle aft flight deck, shown in Fig. 6, was used for the RMS ADA study.

The RMS ADA study used a Shuttle dynamics model, which included flight control system software, a high-fidelity RMS dynamics model,[11] and a model of the SPAS-02 satellite. The highest fidelity scene generator available was used to provide visual cues for RMS operators. Models of an accelerometer on the RMS and the ADA algorithm were added to SES for this study as described subsequently.

Active Damping Augmentation Implementation in the Systems Engineering Simulator

ADA implementation in the SES was performed in two phases. First, the simulated accelerometer was implemented in the RMS dynamics module and validated against the implementation in the DRS. Next, the ADA modifications to the RMS control system were made, and a Butterworth filter was added to the dynamics module. The system was again validated against the DRS and subsequent engineering and crew studies were performed.

Phase I: Accelerometer Implementation

To model the accelerometer, RMS hinge forces (forces exerted by one arm link on an adjoining link at the joint connecting the two links) were required. These calculations were added to the dynamics in addition to the equations defining the accelerometers. The major real-time consideration in adding these capabilities was that the synchronization with other tasks was not altered. It was critical to the deterministic dynamic response that each task was completed at the expected time. To assure that the RMS dynamic response was not corrupted by the addition of the accelerometer model, the dynamic response of the ADA configuration dynamics was compared to the current configuration and the software optimized to retain dynamic fidelity.[12]

Phase II: Active Damping Augmentation Controller

As with the accelerometer simulation, the critical real-time consideration in implementing the ADA controller was task timing. The addition of the ADA logic could not add to the control system task length significantly enough to force any of the shared tasks to lose synchronization. To verify that the RMS modification did not affect the simulation, timing runs were made in which the task length of every required task on each computer was monitored. Similar testing was repeated on the RMS dynamics following the implementation of the Butterworth filter.

In the RMS system, information is passed between the RMS motor control hardware and the GPC via the MCIU, which runs every 42 ms. Although the RMS control system and the dynamics are able to communicate through shared memory in the SES, care

is taken to model the real-world-time lags. The loop time between GPC command issuance and receipt of response is the same as in the actual hardware.

Validation testing was performed comparing the DRS and SES controller implementation. Both open- and closed-loop tests were performed. After initial inconsistencies in payload related parameters were resolved, the comparison data were judged acceptable.

Operator controlled ADA activation and deactivation from the cockpit was provided for engineering assessment. An existing switch in the Shuttle cockpit simulator was used for this purpose.[13]

VI. Results

Preliminary Evaluation

Following an independent validation of the compensator implementation logic and the simulated RMS triaxial accelerometer, ADA point-design controllers were implemented and tested in the SES. Six point-design compensators were synthesized using the techniques summarized in Sec. IV. Of the six control laws, five provided a noticeable improvement in the RMS vibratory response following

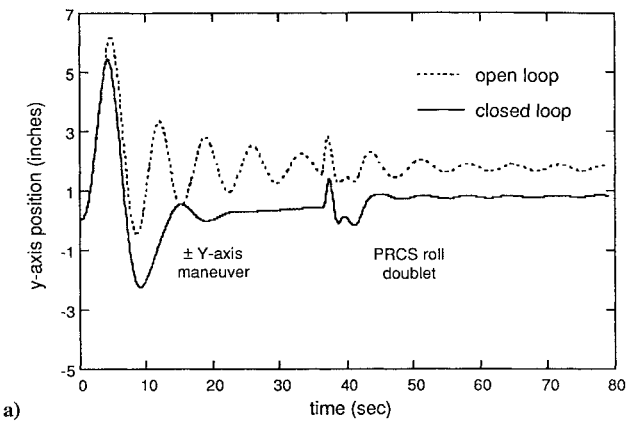

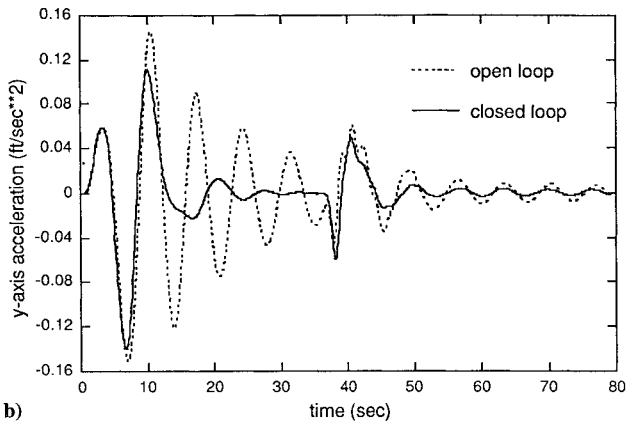

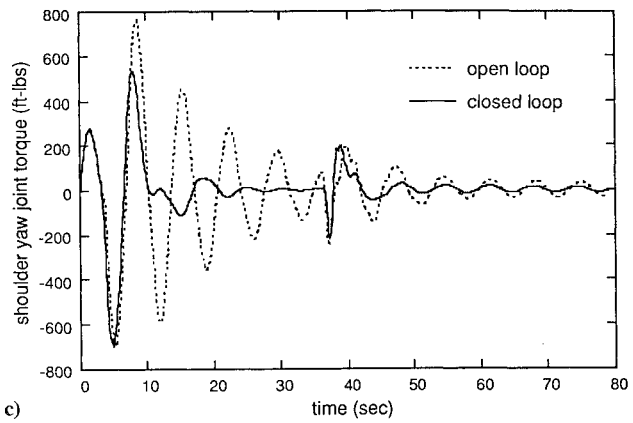

Fig. 7 Phase 2a results: a) position, b) acceleration, and c) torque.

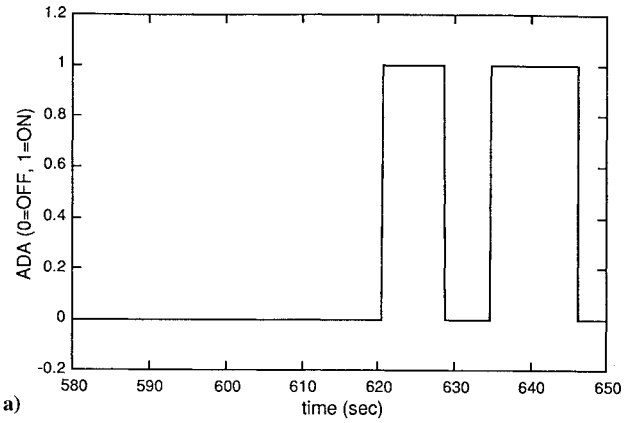

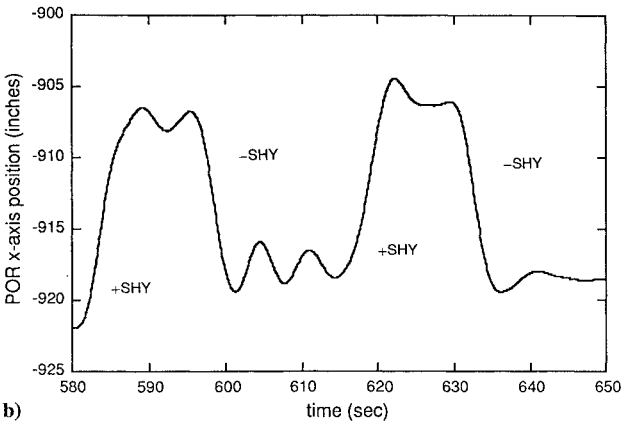

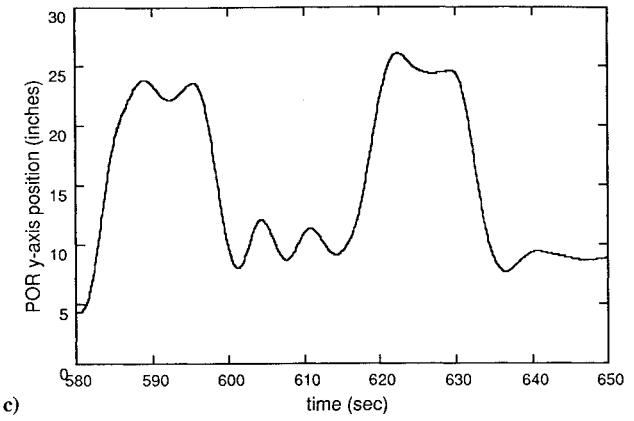

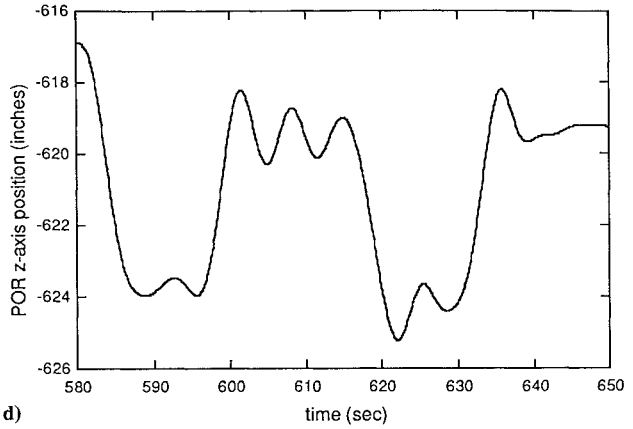

Fig. 8 Astronaut evaluation of ADA: a) ADA activation flag, b) POR x-axis position, c) POR y-axis position, and d) POR z-axis position.

full-scale hand controller commands and Shuttle thruster firings. One control law required loop-gain reduction to achieve stable performance.

The performance of a single point-design compensator derived using the gradient-based optimization method for the low hover arm configuration is summarized in Fig. 7. The open- vs closed-loop responses (i.e., with and without ADA) of the RMS/payload system to a 3 s ± y-axis command to the translational hand controller followed by a 1-s ± roll command (initiated at $t \approx 38$ s) to the Shuttle primary reaction control system (PRCS) thrusters are shown. The open- and closed-loop responses were simulated independently with manual inputs made by an operator in the aft cockpit of the SES using an event timer. The plots of y-axis tip position and acceleration demonstrate the improved damping of the RMS following the manual mode maneuver as well as disturbance rejection of the thruster doublet. Also shown is a plot of the open- vs closed-loop shoulder yaw torque that demonstrates the capability of ADA to reduce loads on the RMS.

The performance of ADA global control laws developed using GBO design techniques were verified in the SES using PTIs. These PTIs allowed for repeatable open- vs closed-loop maneuvers and jet firing responses to be evaluated. Quantitative performance measurements were derived from recorded simulator data and based on this quantitative assessment, a single global controller was selected for the astronaut evaluation of ADA.

Astronaut Evaluation

Six RMS trained astronauts participated in the qualitative evaluation of the effectiveness and utility of ADA to on-orbit RMS operations. Each astronaut was briefed on the ADA methodology, allotted an hour of simulation time to conduct the evaluation, and encouraged to maneuver over the range of RMS configurations using arbitrary manual and single mode command inputs. They were also invited to use the Shuttle RCS jets to deliberately excite the system.

The responses to repeated single-joint maneuvers, made by an astronaut operator, with and without ADA are shown in Fig. 8. The first set of commands are made without ADA, and the second set is made with ADA (activated at the end of the maneuver) as indicated in Fig. 8a. The maneuvers are ± commands to the shoulder yaw (SHY) joint. The x-, y-, and z-axis position of the point of resolution (POR) (located at the midpoint of a line through the SPAS-02 trunnions above the keel pin) are shown as a function of time in Figs. 8b–8d. Significant reduction in the vibratory response following the maneuvers with ADA is observed in all three axes. Similar results were also demonstrated with manual mode maneuvers and Shuttle thruster firings.

Of the six astronauts who evaluated ADA, three were favorably impressed with the capabilities of ADA to enhance RMS performance whereas the remaining three had generally less favorable impressions. Several of the astronauts provided very thorough engineering evaluations of ADA, identifying improvements in fine positioning of payloads near payload attachment hardware in the Shuttle payload bay as a major operational benefit. The less favorable impressions appear related to crew training and on-orbit operation expressly designed to minimize excitation of RMS oscillations. All six of the astronauts were unanimous in wanting to see the application of ADA to much heavier payloads than considered in the study. Heavier payloads are of concern because RMS oscillations are more apparent and because of the difficulty of maneuvering the very heavy Space Station Freedom segments into position for on-orbit assembly.

VII. Concluding Remarks

ADA has been successfully applied to the Shuttle RMS to reduce the vibration decay time following normal payload maneuvers and operations. Simulation of ADA was conducted in the real-time human-in-the-loop SES at the NASA Johnson Space Center. A qualitative definition of RMS operational performance improvement by astronaut operators and supporting quantitative performance data was obtained. Vibratory motions were sensed using a simulated three-axis accelerometer mounted at the end of the lower boom of the RMS. The sensed motions were used in a feedback control law which generated commands to the joint servo mechanisms to reduce the unwanted oscillations. Active damping of the RMS with an attached 3990-lb payload was demonstrated. Six astronaut operators evaluated the performance of an ADA control law following single-joint and coordinated six-joint translational and rotational maneuvers as well as ADA disturbance rejection of Shuttle thruster firings. Significant reductions in the dynamic response of the 3990-lb payload were observed. Astronaut operators recommended investigation of ADA benefits to heavier payloads where oscillations are of more concern.

Acknowledgments

This study was the result of a very successful collaboration between several different organizations. The authors gratefully acknowledge the individuals at the Charles Stark Draper Laboratory (Cambridge, Massachusetts), Lockheed Engineering and Sciences Company (Houston, Texas, and Hampton, Virginia), and NASA Johnson Space Center (Houston, Texas) for their contributions to this effort.

References

[1]NSTS Integration and Operations Office, Johnson Space Center, "Space Shuttle System Payload Accommodations," NASA NSTS-007700, Vol. XIV, App. 8, Rev. J, Jan. 1988.

[2]Kain, R. A., and Hoefer, S., "Shuttle Flight Operations Manual: Vol. 16—Payload Deployment and Retrieval System," NASA JSC-12770, June 1, 1981.

[3]Gilbert, M. G., Scott, M. A., and Sean, P. K., "Active Damping Augmentation to the Shuttle RMS," Fourth Annual NASA/Dept. of Defense Conf. on Controls–Structures Interaction Technology, NASA-TM-102763, Nov. 1990.

[4]Scott, M. A., Gilbert, M. G., and Demeo, M. E., "Active Vibration Damping of Space Shuttle Remote Manipulator System," *Journal of Guidance, Control, and Dynamics*, Vol. 16, No. 2, 1993, pp. 275–280; also NASA TM-104149.

[5]Juang, J.-N., Phan, M., Horta, L. G., and Longman, R. W., "Identification of Observer/Kalman Filter Markov Parameters: Theory and Experiments," *Journal of Guidance, Control, and Dynamics*, Vol. 16, No. 2, 1993, pp. 320–329.

[6]Phan, M., Horta, L. G., Juang, J.-N., and Longman, R. W., "Linear System Identification Via an Asymptotically Stable Observer," *Proceedings of the AIAA Guidance, Navigation, and Control Conference* (New Orleans, LA), AIAA, Washington, DC, 1991 (AIAA Paper 91-2735).

[7]Juang, J.-N., Horta, L. G., and Phan, M., "System/Observer/Controller Identification Toolbox," NASA TM-107566, Feb. 1992.

[8]Horta, L. G., Phan, M., Juang, J.-N., Longman, R. W., and Sulla, J. L., "Frequency Weighted System Identification and Linear Quadratic Controller Design," *Journal of Guidance, Control, and Dynamics*, Vol. 16, No. 2, 1993, pp. 330–336.

[9]Gupta, N. K., "Frequency-Shaped Cost Functionals: Extension of Linear-Quadratic Gaussian Design Methods," *Journal of Guidance, Control, and Dynamics*, Vol. 3, No. 6, 1980, pp. 529–535.

[10]Gray, C., Koenig, M., Metzinger, R., Reasor, G., and Turnbull, J., "Validation of the Draper RMS Simulation (DRS) Against Flight Data," Charles Stark Draper Lab., CSDL-R-1755, Cambridge, MA, Vol. 1–2, April 1985.

[11]Anon., "Systems Engineering Simulator Remote Manipulator Flight-to-Simulation Validation Report," Lockheed Engineering and Sciences Co., LESC-30028, Houston, TX, May 1992.

[12]Jensen, M. C., "Systems Engineering Simulator (SES) Remote Manipulator System (RMS) Augmented Damping Study Validation Report," Lockheed Engineering and Sciences Co., LESC-30027, Houston, TX, May 1993.

[13]Jensen, M. C., "Systems Engineering Simulator (SES) Requirements Document for the Remote Manipulator System (RMS) Damping Augmentation Study," Lockheed Engineering and Sciences Co., LESC-29879, Houston, TX, Feb. 1992.